Biochemical Pharmacology 82 (2011) 1198–1208

Contents lists available at ScienceDirect

Biochemical Pharmacology

journal homepage: www.elsevier.com/locate/biochempharm

Des-aspartate-angiotensin-I and angiotensin IV improve glucose tolerance and insulin signalling in diet-induced hyperglycaemic mice

Yong-Chiat Wong [a], Meng-Kwoon Sim [a,*], Kok-Onn Lee [b]

[a] Department of Pharmacology, Yong Loo Lin School of Medicine, National University of Singapore, Singapore
[b] Department of Medicine, Yong Loo Lin School of Medicine, National University of Singapore, Singapore

ARTICLE INFO

Article history:
Received 1 June 2011
Accepted 13 July 2011
Available online 23 July 2011

Keywords:
Des-aspartate-angiotensin I
Angiotensin IV
Diet-induced hyperglycaemia
Insulin resistance
Angiotensin receptor type I
Insulin regulated aminopeptidase

ABSTRACT

Although clinical studies suggested that blockade of the renin-angiotensin system may prevent diabetes, the mechanism is uncertain. As a follow-up to an earlier study, we investigated how des-aspartate-angiotensin-1 (DAA-1) and its metabolite, angiotensin IV (Ang-IV) improved glucose tolerance in diet-induced hyperglycaemic mice. Male C57BL/6J mice were fed a high-fat-high-sucrose (HFD) or normal (ND) diet for 52 weeks. HFD animals were orally administered either DAA-I (600 nmol/kg/day), Ang-IV (400 nmol/kg/day) or distilled water. Body weight, blood glucose and insulin were measured fortnightly. Inflammatory and insulin signalling transducers that are implicated in hyperglycaemia were analyzed in skeletal muscles at 52 weeks. HFD animals developed hyperglycemia, hyperinsulinemia and obesity. DAA-I and Ang-IV improved glucose tolerance but had no effect on hyperinsulinemia and obesity. Skeletal muscles of HFD animals showed increased level of ROS, gp91 of NADPH oxidase, pJNK and AT_1R-JAK-2-IRS-1 complex. Both DAA-I and Ang-IV attenuated these increases. Insulin-induced activation of IR, IRS-1, IRS-1-PI3K coupling, phosphorylation of Akt, and GLUT4 translocation were attenuated in skeletal muscles of HFD animals. The attenuation was significantly ameliorated in DAA-I-treated HFD animals. In corresponding Ang-IV treated animals, insulin induced IRAP and PI3K interaction, activation of pAkt and GLUT4 translocation, but no corresponding activation of IR, IRS-1 and IRS-1-PI3 K coupling were observed. DAA-I and Ang-IV improved glucose tolerance, insulin signalling, and para-inflammatory processes linked to hyperglycaemia. DAA-I acts via the angiotensin AT_1 receptor and activates the insulin pathway. Ang-IV acts via IRAP, which couples PI3K and activates the later part of the insulin pathway.

1. Introduction

Angiotensin II (Ang-II) is involved in the pathogenesis of diet-induced hypertension and insulin resistance [1–3]. The angiotensin AT_1 receptor has been shown to couple components of insulin signalling pathway via JAK2 to form JAK/IRS-1/PI3K, and to activate JNK. These two actions result in inhibitory serine phosphorylation of key elements of the insulin-signalling pathway [4–6]. Consistent with these findings, angiotensin converting enzyme inhibitors and angiotensin receptor blockers have been reported to improve insulin resistance in type 2 diabetics [7–9]. Inhibition of the renin angiotensin system (RAS) in the LIFE trial was also associated with a reduction in the risk of new-onset diabetes [10]. Similar association was also seen in the CHARM [11] and VALUE [12] studies. These large randomized clinical trials show a possible causal relationship between increase in RAS activity and diabetes. Tikellis et al. [13] investigated the specific effects of RAS blockade on pancreatic islet structure and function in diabetic rats. They showed that Zucker rats exhibited increased intraislet expression of various components of the RAS in association with fibrosis, apoptosis, and oxidative stress; and these were attenuated after treatment with perindopril or irbesartan. Besides blockade of the RAS, treatment of diabetic animals with angiotensins that exert biological actions opposing those of angiotensin II was also beneficial. Angiotensin-(1-7) antagonizes the actions of angiotensin II [14,15], and in this respect the heptapeptide has been shown to reduce cardiovascular events associated with oxidative stress in diabetic animals [14–16]. Des-aspartate-angiotensin I (DAA-I), a metabolite of angiotensin I that counteracts several actions of Ang-II [17–20] was recently shown to exert hypoglycaemic action by enhancing insulin-induced GLUT4 translocation in type 2 diabetic KKAy mice and GK rats [21]. The effect of angiotensin IV (Ang-IV) on glucose regulation has also been of interest following the identification of

Abbreviations: Akt, protein kinase B; Ang-II, angiotensin II; Ang-IV, angiotensin IV; DAA-I, des-aspartate-angiotensin I; HFD, high-fat-high-sucrose diet; IR, insulin receptor; IRAP, insulin-related aminopeptidase; JAK, Janus kinase; JNK, c-Jun N-terminal kinases; ND, normal diet; PI3K, phosphoinositide 3-kinase; ROS, reactive oxygen species.

* Corresponding author. Tel.: +65 6516 3268; fax: +65 6873 7690.
E-mail address: phcsimmk@nus.edu.sg (M.-K. Sim).

0006-2952/$ – see front matter © 2011 Elsevier Inc. All rights reserved.
doi:10.1016/j.bcp.2011.07.080

insulin-regulated aminopeptidase (IRAP) as the AT_4 receptor that is linked to the pathogenesis of T2DM [22]. IRAP is known to be involved in GLUT4 trafficking and insulin-stimulated glucose uptake into insulin-responsive cells [23,24]. Although IRAP co-translocates with GLUT4 to the cells surface in response to insulin stimulation in adipocytes, cardiomyocytes and skeletal muscle cells [25–27], the ability of IRAP to mediate the actions of Ang-IV and its role in insulin action in peripheral tissues remains largely unknown. On the basis that insulin resistance in skeletal muscle is a hallmark of type 2 diabetes [28–31], the mechanism of improved glucose tolerance of DAA-I and Ang-IV in the skeletal muscles of diet-induced hyperglycaemic mice was investigated in the present study.

2. Materials and methods

2.1. Antibodies and chemicals

Anti-gp91phox, anti-phospho-JNK, anti-insulin Rα, anti-phospho-IRS-1 (Ser307), anti-phospho-Tyrosine, anti-IRS-1, anti-PI 3-kinase p85α, anti-Akt, anti-GLUT4, anti-phospho-Serine, anti-AT_1R, anti-JAK2, goat anti-mouse IgG-HRP, goat anti-rabbit IgG-HRP, donkey anti-goat IgG-HRP, goat anti-mouse IgM-HRP antibodies were purchased from Santa Cruz Biotechnology (Santa Cruz, CA). Anti-JNK 1/2 antibody was obtained from BD Pharmingen (San Diego, CA). Anti-phospho-Akt (Ser473) antibody was purchased from Cell Signalling Technology (Danvers, MA). Anti-IRAP antibody was purchased from Alpha Diagnostic (San Antonio, TX). Anti-β-actin antibody and divalinal angiotensin IV were purchased from Sigma Aldrich (St. Louis, MO). DAA-I and Ang-IV were purchased from Bachem AG (Bubendorf, Switzerland). Indomethacin was purchased from Cayman Chemical Company (Ann Arbor, MI). Losartan was a gift from Merck & Co., Inc. (Whitehouse Station, NJ).

2.2. Animals

Five- to 6-week-old male C57BL/6J male mice were purchased from the National University of Singapore Centre for Animals Resources. The animals were housed in temperature controlled room at 25 ± 1 °C with lighting from 0700 to 1900 h daily. The use of animals in this study was approved by Institutional Animal Care and Use Committee of National University of Singapore.

2.3. Diet

The animals received either normal diet (ND, Specialty Feeds, Australia) or high-fat high-sucrose diet (HFD, Specialty Feeds, Australia) and water *ad libitum*. On a caloric base, the ND consisted of 19% protein, 12% carbohydrates and 4.6% fat (total 13.5 kJ/g), whereas the HFD consisted of 19% protein, 42% carbohydrates and 23% fat (total 20 kJ/g).

2.4. Oral administration of angiotensin peptides

The animals were randomly assigned into groups of 10 animals as follows:

ND control	mice fed with ND plus oral administration of 0.1 ml drinking water/day.
HFD control	mice fed with HFD plus oral administration of 0.1 ml drinking water/day.
HFD+DAA-I (0)	mice fed with HFD plus oral administration of 600 nmol/kg/day DAA-I starting from 0th week of the diet regime.
HFD+Ang-IV (0)	mice fed with HFD plus oral administration of 400 nmol/kg/day Ang-IV starting from 0th week of the diet regime.
HFD+DAA-I (24)	mice fed with HFD plus oral administration of 600 nmol/kg/day DAA-I starting from 24th week of the diet regime.
HFD+Ang-IV (24)	mice fed with HFD plus oral administration of 400 nmol/kg/day Ang-IV starting from 24th week of the diet regime.

The dose of 600 nmol/kg DAA-I was shown to exert maximum hypoglycaemic effect in diabetic animals in a previous study [21], and a preliminary study showed that 400 nmol/kg Ang-IV exerted maximal glucose lowering effect (unpublished findings). Animals were administered 0.1 ml solution of either DAA-I, Ang-IV or distilled water by oral gavage. The food intake of the animals was determined every 4 weeks for a duration of 48 weeks. The calculation of the energy consumed was based on the weight of the food pellet consumed by the animals for a 24-h period. The weight of food pellet consumed was multiplied by the amount of digestible energy (given by the manufacturer) divided by the weight of the animals, and the energy value was expressed as MJ/g/day. After 52 weeks of treatment, the animals were then subjected to acute insulin stimulation and sacrificed for various molecular studies. With this duration of HFD treatment, the prophylactic actions of both angiotensin peptides (concurrent treatment from 0 week) as well as their actions on fully developed hyperglycaemia (concurrent treatment from 24 weeks) could be studied.

2.5. Intraperitoneal administration of losartan, divalinal-Ang-IV, and indomethacin

Five to 6-week old animals fed on a ND and water *ad libitum* were orally administered either DAA-I (600 nmol/kg/day), Ang-IV (400 nmol/kg/day) or vehicle (water) for up to 6 weeks. DAA-I-treated animals were concurrently administered one of the following by intraperitonal injection: losartan (50 nmol/kg/day), divalinal-Ang-IV (300 nmol/kg/day), indomethacin (200 nmol/kg/day). Ang-IV-treated animals were similarly administered losartan or divalinal Ang-IV. Control animals were administered either losartan, divalinal-Ang-IV, or indomethacin. Indomethacin powder was directly dissolved in 0.1 M warm Na_2CO_3 in concentration of 0.1 mg/ml and subsequently diluted to appropriate concentration in PBS (pH 7.2).

2.6. Oral glucose tolerance test (OGTT) and serum insulin determination

At every 4 weeks, the animals were fasted overnight and the weight of individual animals was recorded prior to an oral administration of 2 g/kg glucose solution. Blood was taken from the orbital sinus (10 μl) of each animal immediately before glucose administration, and at 30, 60, and 120 min after glucose administration. The blood was allowed to clot and the serum assayed for glucose and insulin concentration using commercial glucose reagent and insulin kits from Thermo Electron Corp (Victoria, Australia) and Crystal Chem Inc (Downers Grove, IL), respectively.

2.7. Correlation of serum glucose and insulin with insulin resistance

The whole-body insulin sensitivity was calculated based on an equation defined as an index of whole body insulin sensitivity [10,000/square root of (fasting glucose × fasting insulin) × (mean glucose × mean insulin during OGTT)]. This index has been shown to correlate with the rate of whole-body glucose disposal during the euglycemic insulin clamp [32].

2.8. Insulin stimulation and preparation of skeletal muscle

At the end of 52 weeks, the animals were fasted overnight and intraperitoneally administered 40 U/kg of insulin or equivalent volume of PBS, and sacrificed by cervical dislocation 5 min after the administration. The hind limb skeletal muscles (soleus, plantaris, gastrocnemius, and quadriceps) were excised, immediately frozen in liquid nitrogen and stored at −80 °C until used. The skeletal muscle was homogenized as previously described [21]. Skeletal muscle for GLUT4 translocation study were similarly prepared except that the fasted animals were injected 0.5 U/kg insulin and sacrificed 30 min after insulin injection.

2.9. Preparation of skeletal muscle membrane

The plasma membrane fraction of skeletal muscles was prepared by the method previously described [21].

2.10. Immunoprecipitation and immunoblotting

Equal amount of solubilised skeletal muscle protein (1 mg) were incubated overnight at 4 °C in an end-over-end rotor with anti-IR, anti-IRS-1, anti-IRAP, anti-PI3K or anti-AT_1 receptor antibodies to a final concentration of 4 μg per mg of total protein for all antibodies. The immune complex was captured by adding 50 μl protein A-agarose beads purchased from Calbiochem (Darmstadt, Germany) for 4 h at 4 °C. The immune complex-conjugated beads were pelleted at 15,000 × *g* for 1 min at 4 °C and washed five times with lysis buffer to remove nonspecific binding proteins. The beads were then boiled in Laemmli sample buffer for 10 min, and the protein A-agarose beads were removed from the denatured protein by centrifugation at 15,000 × *g* for 1 min at 4 °C as previously described [21]. For immunoblotting, the plasma membrane (10 μg), protein lysate (30–100 μg) and immunoprecipitates were subjected to SDS-PAGE and transferred to nitrocellulose membranes. The membranes were incubated with respective antibodies and then visualized with an ECL detection kit from Thermo Scientific (Waltham, MA) as previously described [21].

2.11. Detection of ROS

Skeletal muscle tissue samples were cut into 20 μm-thick sections using a cryostat and picked up onto gelatin-coated slides. The samples were incubated with 2 μmol/L dihydroethidium (DHE) solution purchased from Biotium (Hayward, CA) for 30 min at 37 °C. DHE was oxidized in the presence of ROS to form ethidium, which bound specifically to DNA in the nucleus and emit red fluorescence. *In situ* detections of ROS in the skeletal muscles of the treated animals were then carried out using fluorescence microscope and the intensity was quantified using Imaging software (Image Processor, New York University).

2.12. Statistical analysis

Data were expressed as mean ± SEM based on independent experiments. Statistical analysis was performed by Student's *t*-test for comparison between means, or one-way analysis of variance (ANOVA, post hoc Fisher's LSD test) for multiple testing. Probability values were considered significant at $P < 0.05$.

3. Results

3.1. DAA-I and Ang-IV effects on glucose tolerance

HFD animals showed significant increase in 30 min OGTT serum glucose after 8 weeks (20.3 ± 0.5 mM for HFD, 14.8 ± 0.5 mM for ND, Fig. 1). Thereafter, the 30 min OGTT serum glucose of the HFD animals continued to rise and remained significantly higher than the corresponding value of ND animals throughout the study. At the end of 48 weeks, this value was 25.5 ± 0.6 mM, which was about fifty percent higher than the value of ND animals (17.1 ± 0.4 mM). Chronic daily oral treatment with DAA-I (600 nmol/kg) attenuated the hyperglycaemia. The attenuation was observed in animals that received DAA-I treatment before as well as after the onset of HFD-induced hyperglycaemia (Fig. 1A and B, respectively). HFD animals that were administered 400 nmol/kg Ang-IV had similar response except that the onsets of improved glucose tolerance action were shorter (Fig. 1C and D). Fig. 1E shows that chronic treatment of DAA-I and Ang-IV had no effect on the fasting serum glucose level of the HFD animals, but significantly improved the glucose uptake at 30, 60 and 120 min after glucose load.

3.2. Body weight, insulin sensitivity index and energy intake

At 48 weeks of the study, HFD animals were almost two fold heavier than ND animals (54.4 ± 1.7 for HFD, 30.2 ± 1.5 g for ND, Table 1). Daily oral administration of DAA-I and Ang-IV starting from week 0 or week 24 of the diet regime did not alter the HFD induced-weight gain. On the other hand, the data show that DAA-I and Ang-IV significantly increase whole-body insulin sensitivity of HFD animals. As the animals had no alternative to the HFD, the magnitude of the increase was modest (42–64% above the value of untreated HFD animals). This increase was not accompanied by an increase in blood insulin level. The energy intake was greater in HFD animals when compared with the ND animals, and neither DAA-I nor Ang-IV affect the intake (see Table 1 for value at 48 weeks). Significant increase in energy intake occurred from 32 to 48 weeks (data not shown).

3.3. Actions of DAA-I and Ang-IV on insulin signalling

Skeletal muscles of animals fed on HFD for 52 weeks showed increased basal serine phosphorylated IR, and reduced insulin-stimulated tyrosine phosphorylation of IR (Fig. 2A). DAA-I but not Ang-IV significantly attenuated the impairment (Fig. 2B and C). Similarly, skeletal muscles of HFD animals showed increased basal serine phosphorylation of IRS-1 and reduced insulin-stimulated tyrosine phosphorylation of IRS-I (Fig. 3A). In addition, insulin-stimulated coupling of IRS-1 to PI3K was also attenuated. DAA-I but not Ang-IV significantly improved the impairment (Fig. 3B–D). Unlike tyrosine phosphoryaltion, serine phosphorylation of IRS-1 did not appear to be insulin sensitive (see Fig. 3B and C). This was probably due to long onset of Ser-307 phosphorylation of IRS-1 (30 min–120 min after insulin stimulation) [33]. For this reason, insulin stimulation did not bring about the immediate increase of Ser-307-IRS-1 phosphorylation in all animal groups in Fig. 3B, as the animals were sacrificed 5 min post insulin administration.

3.4. Actions of DAA-I and Ang-IV on GLUT4 translocation

Skeletal muscles of HFD showed a greater than 50% decrease in basal and insulin-stimulated serine phosphorylated Akt (activated Akt). Both DAA-I and Ang-IV completely attenuated the decrease (Fig. 4A). In conjunction to the reduction of activated Akt, the insulin-stimulated GLUT4 translocation was impaired in HFD animals. Both DAA-I and Ang-IV attenuated the impairment (Fig. 4B). The basal cell surface GLUT4 remained unchanged in HFD animals, and had been similarly report in HFD rats [34] and diabetic animals [21].

3.5. Actions of DAA-I and Ang-IV on oxidative stress and JNK activation

Skeletal muscles of HFD animals showed an almost six-fold increase in tissue ROS (Fig. 5A and B). DAA-I and Ang-IV treated

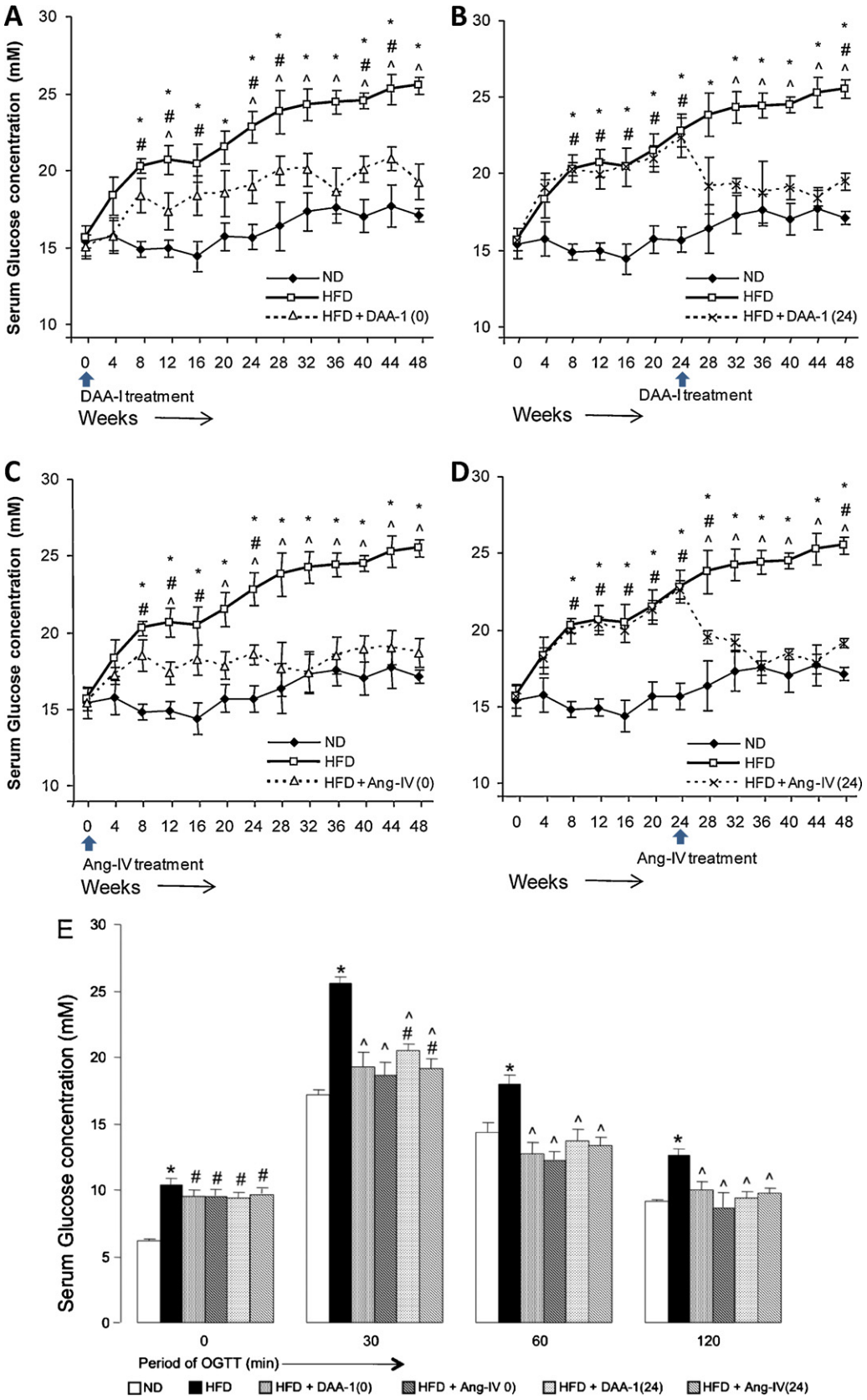

Fig. 1. Effects of DAA-I and Ang-IV on OGTT profile in C57BL/6J mice fed on HFD. Profile of 30 min OGTT where DAA-I was administered on Week 0 (A) and on Week 24 (B). Profile of 30 min OGTT where Ang-IV was administered at Week 0 (C) and on Week 24 (D). Multi-temporal (0, 30, 60 and 120 min) OGTT profile at the end of 48 week (E). Each value is the mean ± SEM obtained from 10 animals. *HFD significantly higher than ND. #HFD + DAA-I or Ang-IV significantly higher than ND. ^HFD + DAA-I or Ang-IV significantly lower than HFD ($P < 0.05$, one way ANOVA, Fisher's LSD).

Table 1
Glycemic characteristics and insulin sensitivity index of HFD mice treated with angiotensin peptides.

Measured parameters	ND	HFD	HFD + DAA-1(0)	HFD + Ang-IV(O)	HFD + DAA-1(24)	HFD + Ang-IV(24)
Body weight (g)	30.2 ± 1.5	54.4 ± 1.7*	51.9 ± 1.0*	51.6 ± 1.3*	53.5 ± 0.9*	51.9 ± 2.0*
Energy intake (Mj/g/day)	52.1 ± 2.1	67.4 ± 3.3*	68.9 ± 2.6*	69.3 ± 3.1*	67.2 ± 2.8*	67.9 ± 2.9*
Fasting blood glucose (mM)	6.1 ± 0.5	10.4 ± 0.4*	9.5 ± 0.4*	9.5 ± 0.5*	9.4 ± 0.3*	9.7 ± 0.3*
OGTT 30 min blood glucose (mM)	17.1 ± 0.4	25.5 ± 0.6*	19.3 ± 1.1#	18.7 ± 1.0#	19.5 ± 0.5*#	19.1 ± 0.7*#
OGTT 120 mm blood glucose (mM)	9.2 ± 0.1	12.5 ± 0.6*	10.0 ± 0.6#	8.7 ± 1.0#	9.4 ± 0.5#	9.7 ± 0.4#
G: [Mean blood glucose of 120 min OGTT (mM)]	10.9 ± 0.3	16.4 ± 0.2*	12.8 ± 0.3*#	12.2 ± 0.5*#	12.8 ± 0.2*#	12.3 ± 0.1*#
Fasting blood insulin (ng/ml)	0.4 ± 0.1	1.3 ± 0.2*	1.2 ± 0.2*	1.1 ± 0.2*	1.6 ± 0.3*	1.4 ± 0.3*
OGTT 60 min blood insulin (ng/ml)	0.2 ± 0.1	1.2 ± 0.3*	0.8 ± 0.1*	0.8 ± 0.1*	1.3 ± 0.2*	1.3 ± 0.1*
I: [Mean blood insulin of 120 min OGTT (ng/ml)]	0.4 ± 0.1	1.4 ± 0.2*	0.9 ± 0.1*	1.0 ± 0.1*	1.2 ± 0.1*	1.3 ± 0.1*
Insulin sensitivity index	3219 ± 316	620 ± 96*	944 ± 75*#	1018 ± 122*#	1011 ± 94*#	884 ± 86*#
AUC (0 min–120 min) (mM)	1523 ± 87	2027 ± 142*	1589 ± 186*#	1511 ± 190*#	1657 ± 131*#	1611 ± 122*#

Values represent mean ± SEM obtained from 10 individual animals at the end of 48 weeks.
Insulin sensitivity index = $10{,}000/\{([\text{glucose}]_{0\ \text{min}} \times [\text{insulin}]_{0\ \text{min}} \times (G \times I))\}^{1/2}$. G = mean blood glucose of 120 min OGTT; I = mean blood insulin of 120 min OGTT.
* Significantly different from the value of ND.
\# Significantly different from the value of HFD.

animals were found to have significantly lesser skeletal muscle ROS. Similar trend and effect of DAA-I and Ang-IV was seen with gp91 of NADPH oxidase (Fig. 5C) and activation of JNK (Fig. 5D).

3.6. Actions of DAA-I and Ang-IV on association of JAK-2 and IRS-1 to AT_1 receptor and insulin-stimulated IRAP-PI3K interaction

Skeletal muscles of HFD animals showed a four-fold increase in coupling of IRS-1 and JAK-2 to the angiotensin AT_1 receptor at basal level. This increase was significantly attenuated in DAA-I treated animals and to a lesser extent in Ang-IV treated animals (Fig. 6A–C). Skeletal muscles of HFD animals treated with Ang-IV showed coupling of IRAP to PI3K upon insulin stimulation. The coupled IRAP was also tyrosine phosphorylated (Fig. 6D)

3.7. Effects of losartan, divalinal-Ang-IV and indomethacin on hypoglycaemic actions of DAA-1 and Ang-IV

C57BL/6J mice administered DAA-I or Ang-IV for 6 weeks showed a significant drop in 30 min OGTT blood glucose. Concurrent treatment with losartan or indomethacin attenuated the hypoglycaemic action of DAA-I. Similarly, the hypoglycaemic action of Ang-IV was attenuated by concurrent treatment of divalinal Ang-IV but not indomethacin (Fig. 7). At the doses used,

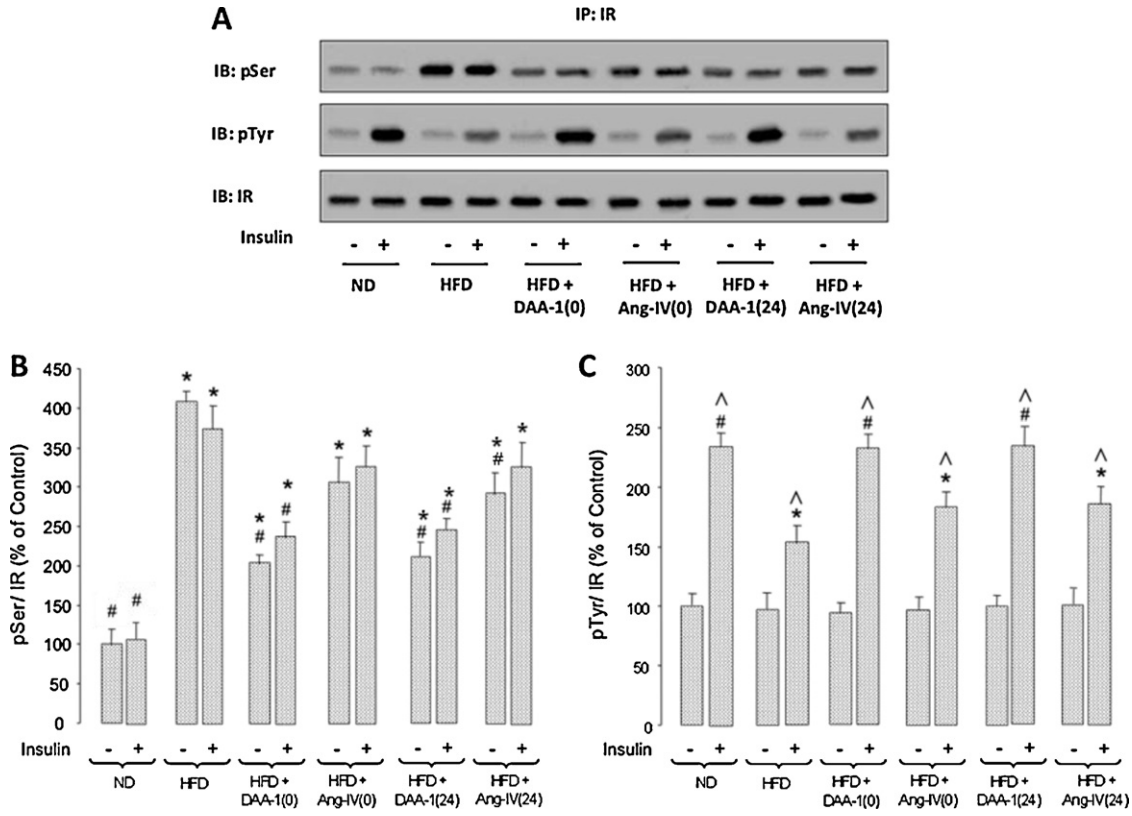

Fig. 2. Effects of DAA-I and Ang-IV on insulin-stimulated activation of IR in skeletal muscle of C57BL/6J mice fed on HFD. (A) Representative data of Western blot proteins immunoprecipitated (IP) with antibody of IR, and immunoblotted (IB) with pSer, pTyr or IR antibodies. (B) Phosphoserine IR protein content. (C) Phosphotyrosine IR protein content. The vertical bars represent the SEM of samples obtained from 3 individual animals, assigning a value of 100% to the non-insulin treated ND control. *Significantly different from corresponding animals fed with ND. #Significantly different from corresponding animals fed with HFD ($P < 0.05$, one way ANOVA, Fisher's LSD). ^Significantly different between the non-insulin-treated and insulin-treated animals ($P < 0.05$, two-tailed t test).

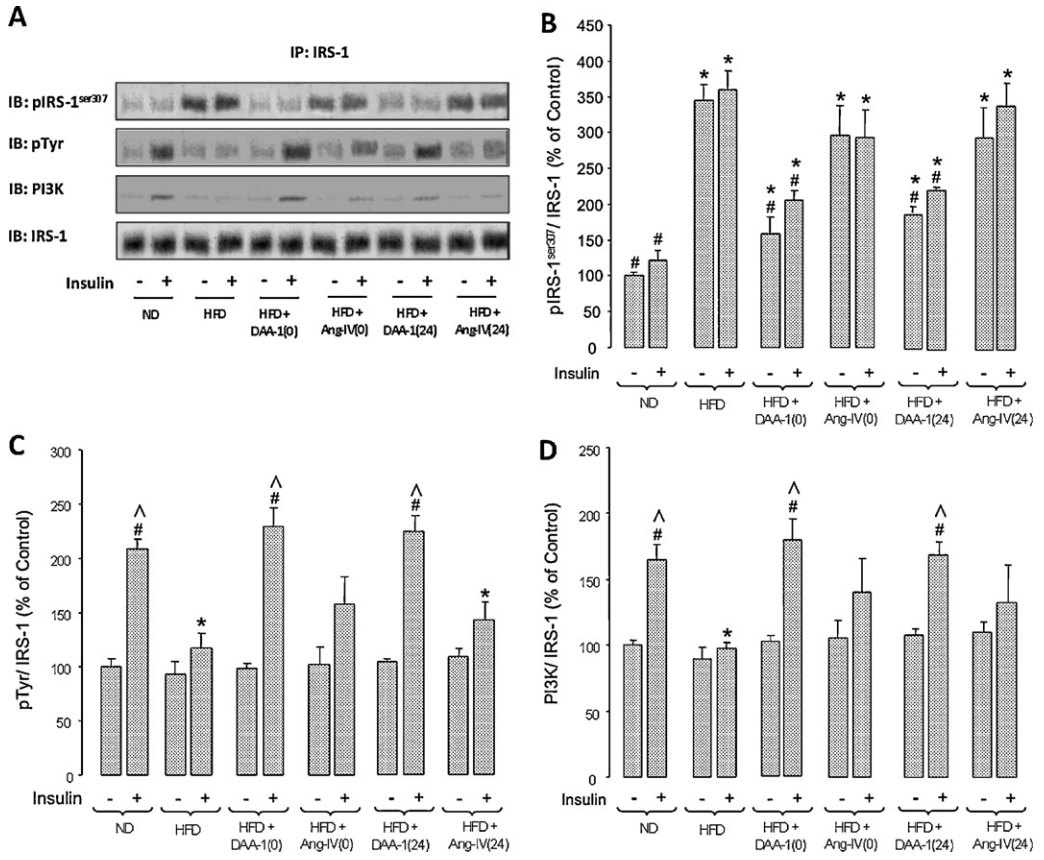

Fig. 3. Effects of DAA-I and Ang-IV on insulin-stimulated activation of IRS-1 in skeletal muscle of C57BL/6J mice fed on HFD. (A) Representative data of Western blot proteins immunopecipitated (IP) with antibody of IRS-1 and immunoblotted (IB) with pIRS-1^{ser307}, pTyr, PI3K or IRS-1 antibodies. (B) Phosphoserine^{307} IRS-1 protein content. (C) Phosphotyrosine IRS-1 content. (D) Content of PI3K that was coupled to IRS-1. The vertical bars represent the SEM of samples obtained from 3 individual animals, assigning a value of 100% to the non-insulin treated ND control. *Significantly different from corresponding animals fed with ND. #Significantly different from corresponding animals fed with HFD ($P < 0.05$, one way ANOVA, Fisher's LSD). ^Significantly different between the non-insulin-treated and insulin-treated animals ($P < 0.05$, two-tailed t test).

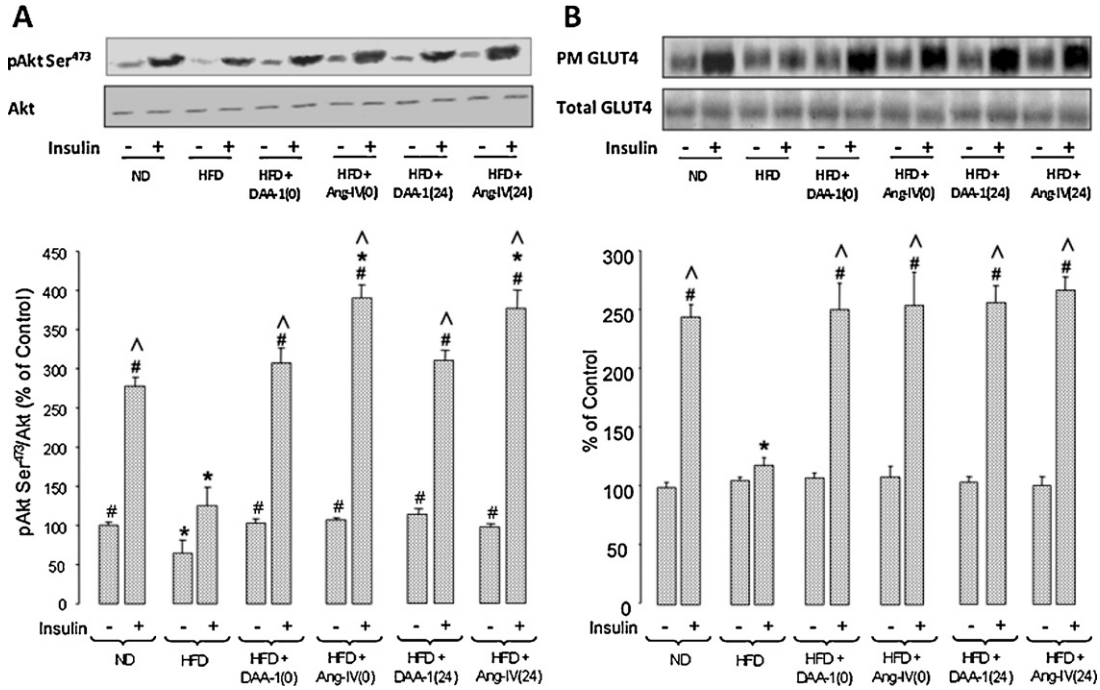

Fig. 4. Effects of DAA-I and Ang-IV on insulin-stimulated activation of pAkt and GLUT4 translocation in skeletal muscle of C57BL/6J mice fed on HFD. (A) Upper panel, Representative data of Western blot protein for pAkt and Akt; Lower panel, Phosphoserine^{473} Akt content. (B) Upper panel, representative data of Western blot for GLUT4 protein from plasma membrane (PM) and crude membrane (total); lower panel, plasma membrane GLUT4 content. The vertical bars represent the SEM of samples obtained from 3 individual animals, assigning a value of 100% to the non-insulin treated ND control. *Significantly different from corresponding animals fed with ND. #Significantly different from corresponding animals fed with HFD ($P < 0.05$, one way ANOVA, Fisher's LSD). ^Significantly different between the non-insulin-treated and insulin-treated animals ($P < 0.05$, two-tailed t test).

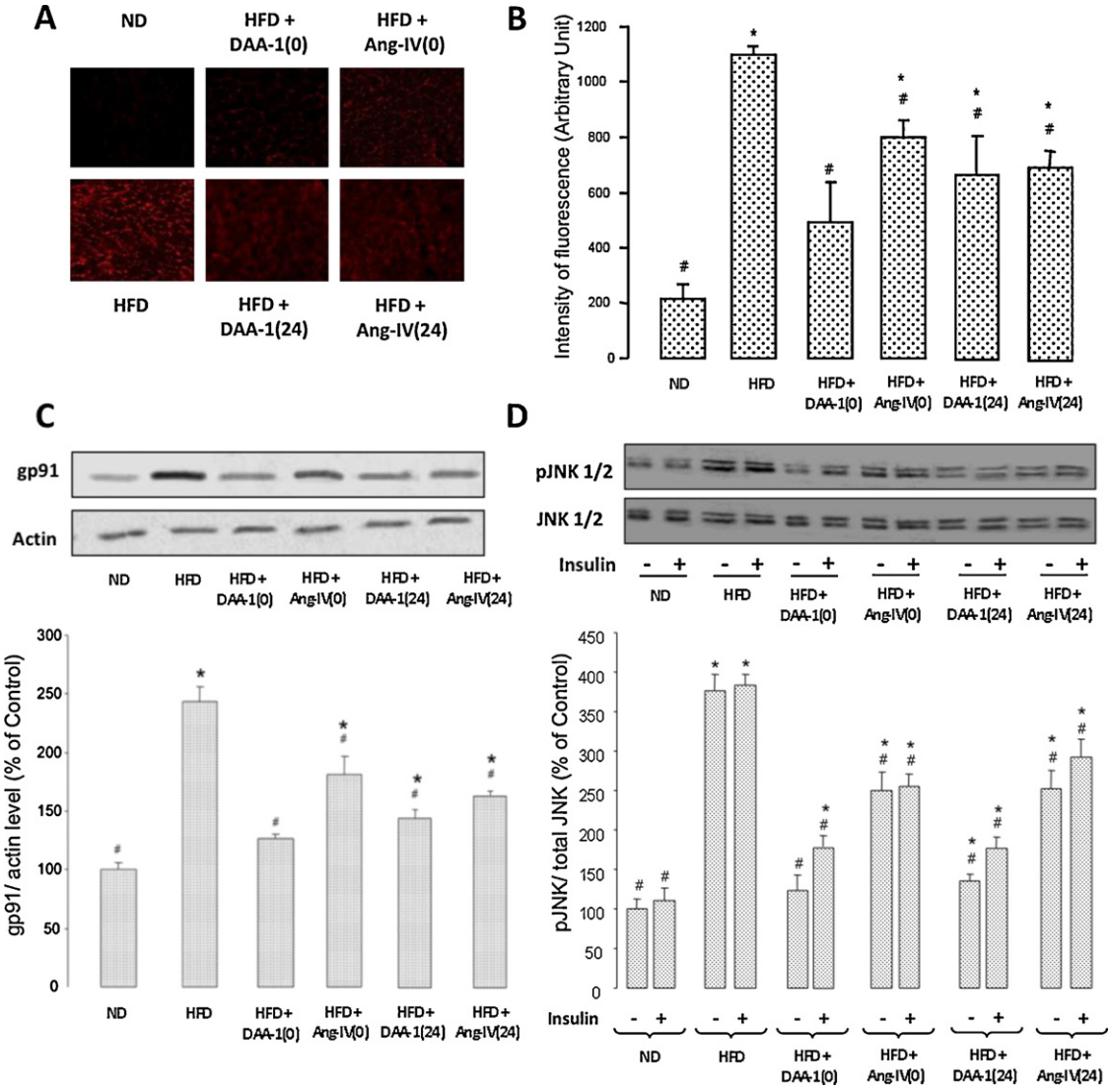

Fig. 5. Effects of DAA-I and Ang-IV on ROS formation, gp91 of NADPH oxidase expression and JNK activation in skeletal muscle of C57BL/6J mice fed on HFD. (A) Representative data of *in situ* detection of ROS in skeletal muscle. (B) Quantitative fluorescence data of A. The vertical bars represent the SEM of samples obtained from 6 individual animals. (C) Upper panel, Representative data of Western blot for gp91 of NADPH oxidase and actin; lower panel, gp91 protein content expressed against the actin content. (D) Upper panel, Representative data of Western blot for pJNK 1/2 and JNK 1/2 proteins; lower panel, ratio of phosphoserine JNK 1/2: JNK 1/2. The vertical bars represent the SEM of samples obtained from 3 individual animals, assigning a value of 100% to the ND control. *Significantly higher than ND. #Significantly lower than HFD control group ($P < 0.05$, one way ANOVA, Fisher's LSD).

losartan, indometahcin, and divalinal Ang-IV had no effect on the blood glucose of the normal healthy animals.

4. Discussion

C57BL/6J mice were chosen for this study as this strain of mice was differentially sensitive to dietary manipulations [35–37] and had been extensively used in diabetes studies [38,39]. Impairment in insulin-induced glucose transport in skeletal muscle has been well documented [28–30], and the skeletal muscle was chosen to study the mechanism of glucose tolerance of the two peptides. As demonstrated in earlier studies, nanomolar concentrations of DAA-I when administered orally, have been shown to be effective in animal models of various pathologies [40–43], including diabetes [21]. This is due to it being effective at nanomolar range, which is a 1000-fold lower than the Michaelis–Menten constant (K_m) of most enzymes.

Significant increase in body weight, blood glucose and insulin, and decrease in insulin sensitivity were found to occur in the animals after 4 weeks of feeding on a HFD. Similar findings were also reported in an earlier study by Prada et al. [44]. Chronic daily oral treatment of DAA-I (600 nmol/kg) and Ang-IV (400 nmol/kg) attenuated the hyperglycaemia and improved insulin sensitivity in the HFD animals without affecting their body weight. This effect was observed in the HFD animals that received the angiotensin peptides treatment before and after the onset of diet-induced hyperglycaemia (starting from week 0 and 24, respectively). Notably, both angiotensin peptides were not insulin secretagogues and improved glucose tolerance in HFD animals by attenuating insulin resistance.

HFD animals suffered from impaired insulin-stimulated tyrosine phosphorylation of IR and IRS-1, IRS-1/PI3K association, Akt activation and GLUT4 translocation. Similar defects had been reported in related studies [44–47]. DAA-I treatment significantly improved these impairments showing that it acted by modulating the phosphorylation and interaction of IRS-1 and kinases of the insulin pathway. The action of DAA-I on insulin-stimulated tyrosine phosphorylation of IRS-1 and

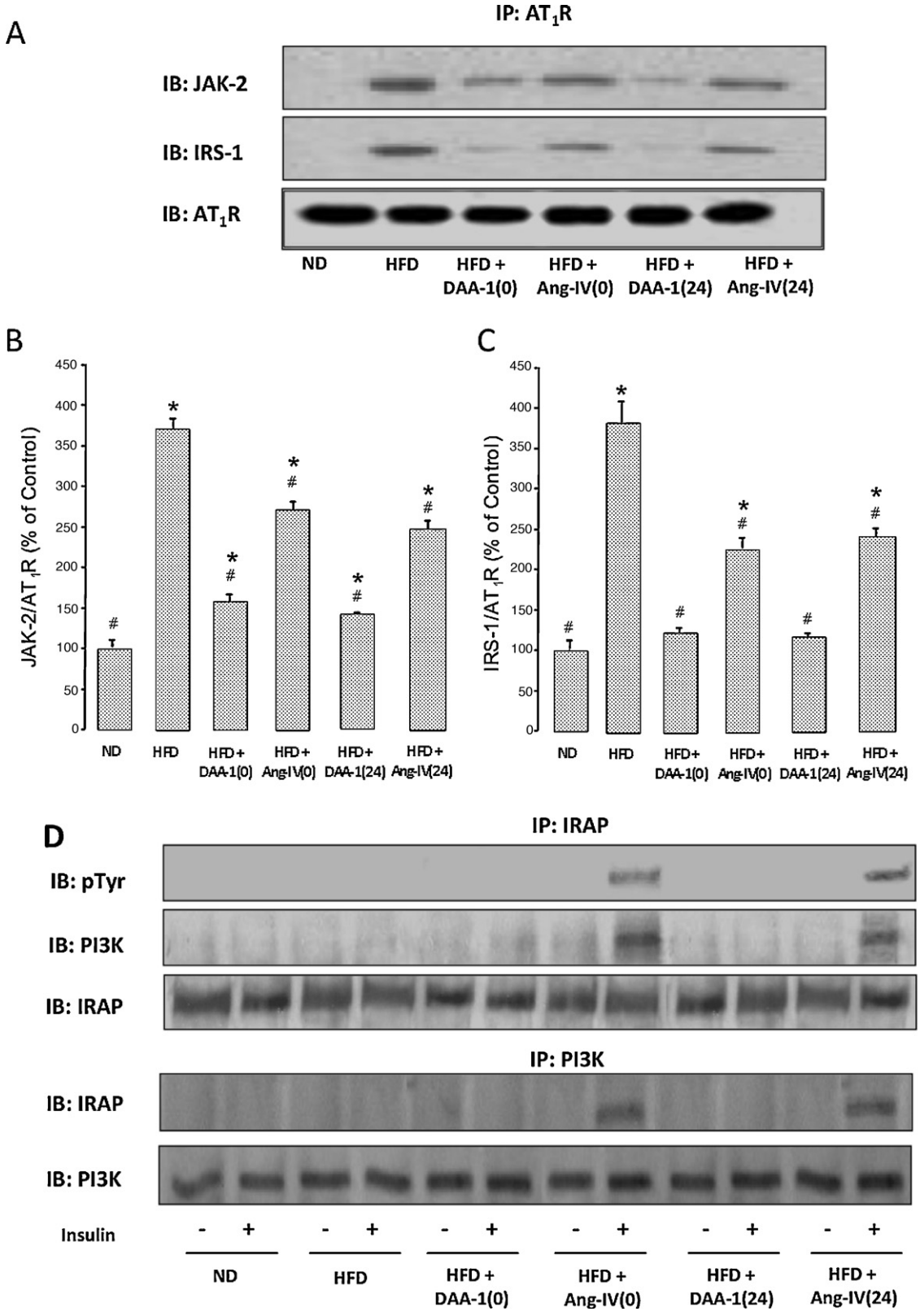

Fig. 6. Effects of DAA-I and Ang-IV on association of JAK-2 and IRS-1 to AT_1 receptor at basal level, and insulin-stimulated IRAP-PI3K interaction in skeletal muscle of C57BL/6J mice fed on HFD. (A) Representative data of Western blot proteins immunoprecipitated (IP) with antibody against AT_1 receptor, and immunoblotted (IB) with JAK-2, IRS-1 and AT_1 receptor antibodies. (B) JAK-2 against AT_1 receptor protein content. (C) IRS-1 against AT_1 receptor protein content. The vertical bars represent the SEM of samples obtained from 3 individual animals, assigning a value of 100% to the ND control. *Significantly higher than ND. #Significantly lower than HFD control group ($P < 0.05$, one way ANOVA, Fisher's LSD). (D) Upper panel, representative data of Western blot proteins immunoprecipitated (IP) with IRAP antibody and immunoblotted (IB) with pTyr, PI3K and IRAP antibodies. Lower panel, representative data of Western blot proteins immunopecipitated (IP) with PI3K antibody and immunoblotted (IB) with IRAP and PI3K antibodies.

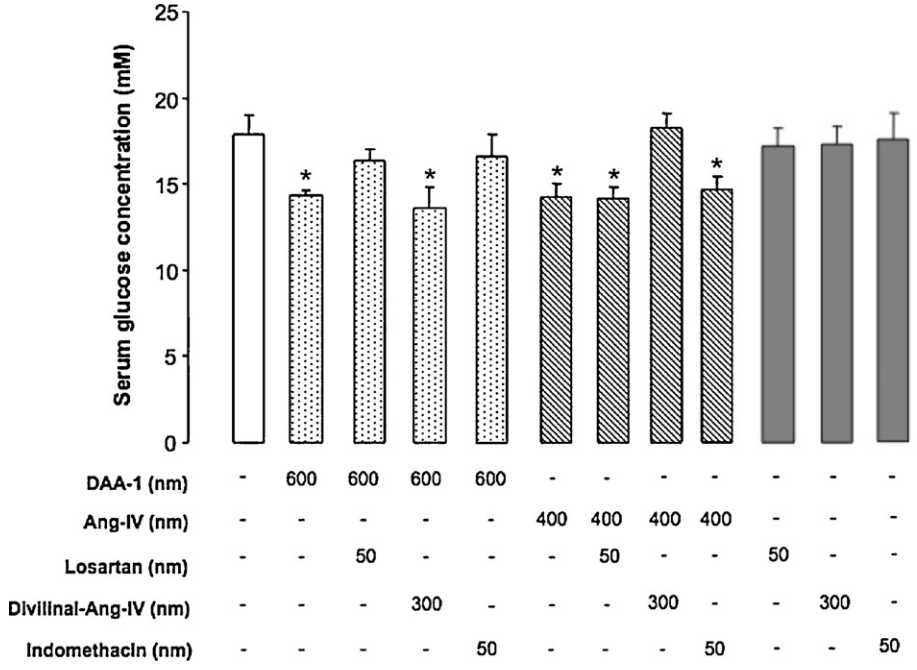

Fig. 7. Effects of AT_1 and AT_4 receptor blockers and indomethacin on hypoglycaemic actions of DAA-I and Ang-IV in C57BL/6J mice. The profile of 30 min OGTT was determined in animals that were treated with either DAA-1 or Ang-IV in the absence and presence of blockers and indomethacin for a period of 6 weeks. The effect of the blockers and indomethacin at the dose used were also studied. The vertical bars represent the SEM of mean values obtained from 10 individual animals. *Significantly lower than the value of untreated animals ($P < 0.05$, one way ANOVA, Fisher's LSD).

GLUT4 translocation had been reported in KKAy mice and GK rats [21].

HFD also increased serine phosphorylation of IR and IRS-1, ROS formation, expression of gp91 protein, and activated JNK, and these elevated parameters were significantly attenuated in HFD animals that were treated with DAA-I. DAA-I has been shown to act as an agonist on the AT_1 receptor and exerts actions opposing those of Ang-II [18,21,48,49], and these could include (i) the Ang-II-induced ERK1/2 and JNK activation that resulted in serine phosphorylation of IR and IRS-1 and impairment of insulin early signal transduction [50] (ii) inhibition of insulin signalling and insulin-stimulated glucose transport in isolated mammalian skeletal muscle that is partially mediated by ROS [51]. HFD animals exhibited increased basal formation of AT_1R/JAK-2/IRS-1, and this could be one of the causes of the hyperglycaemia seen in these animals. The involvement of Ang-II in this formation and its effect on the curtailment of insulin action had been reported [4,5,52]. DAA-I attenuated the basal association of IRS-1/JAK to AT_1 receptor.

The hypoglycaemic action of DAA-I in C57BL/6J mice had been reported in an earlier study [21], and this observation was used to study the specific receptor that mediated the action of DAA-I and Ang-IV, respectively. ND mice were used instead of HFD because angiotensin receptor blockers including losartan have been shown to affect the pathology of type 2 diabetic animals and humans [53,54], and the effect of divalinal-Ang-IV in diabetic animals, if any, is not known. In addition, the effect of indomethacin could not be studied as concurrent administraion of indomethacin to HFD animals for period up to 8 weeks caused fatality (data not shown). The action of DAA-1 in ND mice was blocked by concurrent treatment with either losartan or indomethacin, which, at the dose of 50 nm/kg, had no effect on the fasting blood glucose level of the animals. This data are in agreement with earlier findings showing that the action of DAA-I is mediated by the angiotensin AT_1 receptor and involved prostaglandins as second messengers [18,40,41,43]. Prostaglandins are ligands of PPARγ and their actions include potentiation of insulin action and attenuation of inflammatory cytokines and ROS formation [55–58], which could contribute to the hypoglycaemic action seen in HFD animals treated with DAA-I. The hypoglycaemic action of Ang-IV was blocked by divalinal-Ang-IV, an Ang-IV receptor antagonist [59], and not by losartan indicating that Ang-IV acts via the Ang-IV receptor, which has been characterized as IRAP [60]. This observation is in concurrence with the actions of Ang-IV described below.

Ang-IV treatment enhanced insulin-stimulated Akt activation and GLUT4 translocation in skeletal muscles of HFD animals. This occurred in the absence of significant improvement of insulin-stimulated tyrosine phosphorylation of IR and IRS-1, and IRS-1/PI3K association. The inhibitory effects of Ang-IV on serine phosphorylation of IR and IRS-1, ROS formation and JNK activation were also lesser compared to those of DAA-I. These findings suggest that Ang-IV improves insulin sensitivity by targeting components beyond the conventional insulin signalling pathway. Ang-IV also inhibits HFD-induced JAK-2 and IRS-1 attachments to AT_1 receptor, and again to a lesser extent when compared to DAA-I. The ability of Ang-IV to act via the AT_1 receptors is seen in the control of kidney blood flow where higher doses of Ang-IV mediate a decrease in renal blood flow through AT_1 receptor [61,62], and lower doses increase renal blood flow through AT_4 receptor [63,64]. This shows that Ang-IV acts as an agonist of the AT_1 receptor in micromolar range but elicits physiological responses that are independent of AT_1 receptors in nanomolar concentrations. Hence, the other actions of Ang-IV appear to involve the attenuation of oxidative stress that were mediated by the AT_1 receptors.

Ang-IV enhanced insulin-induced tyrosine phosphorylation of the IRAP, and the phosphorylation was accompanied by PI3K attachment suggesting that Ang-IV acts via IRAP, which binds and stimulates PI3K leading to the activation of Akt and glucose uptake. Evidence supporting this suggestion is seen in A-MEC, an endometrial carcinoma cell line, where insulin stimulation resulted in an overexpression of IRAP, PI3K protein, Akt activation, and glucose uptake [65]. Similarly, Ang-IV was found to stimulate

PI3K and induced Akt activation in lung endothelial cells [66]. Phosphoinositide-binding domains like PX, PH and FYVE are not found on IRAP [67,68] and it is unclear how IRAP and PI3K interact, although the binding via an intermediate molecule having such a domain remains a possibility. IRAP co-translocates with GLUT4 to the cells surface in response to insulin stimulation. Several reports suggested that tyrosine and serine amino acids near the dileucine motif of IRAP undergo phosphorylation by protein kinase C-zeta upon insulin stimulation, leading to modification of the motif [24,69]. These changes in the dileucine motif of IRAP disrupt its interaction with acyl-coenzyme a dehydrogenase (ACD), and the dissociation of ACD from IRAP was found to coincide with IRAP/GLUT4 translocation to the plasma membrane. By enhancing insulin-stimulated tyrosine phosphorylation of IRAP, Ang-IV could either enhance the translocation or prolonged the exposure of GLUT4 at the cell surface; both these actions would result in facilitation of glucose uptake. With this pathway of action, the role played by IRS-I is bypassed. This could account for the absence of significant effect on the coupling of PI3K to IRS-1 in response to insulin in Ang-IV-treated animals.

In summary, the present study shows that DAA-I improves glucose tolerance in diet-induced hyperglycaemic mice, and supports similar action seen in diabetic rats and mice [21]. The improved glucose tolerance was brought about by its action on the angiotensin AT_1 receptor. The angiotensin AT_1 receptor in these hyperglycaemic mice was involved in mediating chronic inflammatory processes that were also attenuated by DAA-I. The findings also show that DAA-I is effective when given before and after the onset of hyperglycaemia indicating that it could be an effective prophylactic glucose level-lowering agent. Similar findings were obtained with Ang-IV, albeit via a different pathway that involved tyrosine phosphorylation of IRAP, increased IRAP-PI3K interaction and increased Akt activation. This pathway bypassed the earlier part of the insulin signalling pathway involving IR and IRS-1.

Acknowledgement

The research was supported by grant R-184-000-121-112 from the Nation University of Singapore.

References

[1] Dobrian AD, Davies MJ, Prewitt RL, Lauterio TJ. Development of hypertension in a rat model of diet-induced obesity. Hypertension 2000;35:1009–15.
[2] Farah V, Elased KM, Morris M. Genetic and dietary interactions: role of angiotensin AT1a receptors in response to a high-fructose diet. Am J Physiol Heart Circ Physiol 2007;293:H1083–9.
[3] Kouyama R, Suganami T, Nishida J, Tanaka M, Toyoda T, Kiso M, et al. Attenuation of diet-induced weight gain and adiposity through increased energy expenditure in mice lacking angiotensin II type 1a receptor. Endocrinology 2005;146:3481–9.
[4] Eguchi S, Numaguchi K, Iwasaki H, Matsumoto T, Yamakawa T, Utsunomiya H, et al. Calcium-dependent epidermal growth factor receptor transactivation mediates the angiotensin II-induced mitogen-activated protein kinase activation in vascular smooth muscle cells. J Biol Chem 1998;273:8890–6.
[5] Ishida M, Marrero M, Schieffer B, Ishida T, Bernstein K, Berk B. Angiotensin II activates pp60c-src in vascular smooth muscle cells. Circ Res 1995;77:1053–9.
[6] Carvalheira J, Calegari V, Zecchin H, Nadruz WJ, Guimarães R, Ribeiro E, et al. The cross-talk between angiotensin and insulin differentially affects phosphatidylinositol 3-kinase- and mitogen-activated protein kinase-mediated signaling in rat heart: implications for insulin resistance. Endocrinology 2003;144:5604–14.
[7] Barnett AH, Bain SC, Bouter P, Karlberg B, Madsbad S, Jervell J, et al. Angiotensin-receptor blockade versus converting-enzyme inhibition in type 2 diabetes and nephropathy. N Engl J Med 2004;351:1952–61.
[8] Brenner BM, Cooper ME, de Zeeuw D, Keane WF, Mitch WE, Parving HH, et al. Effects of losartan on renal and cardiovascular outcomes in patients with type 2 diabetes and nephropathy. N Engl J Med 2001;345:861–9.
[9] Lewis EJ, Hunsicker LG, Clarke WR, Berl T, Pohl MA, Lewis JB, et al. Renoprotective effect of the angiotensin-receptor antagonist irbesartan in patients with nephropathy due to type 2 diabetes. N Engl J Med 2001;345:851–60.
[10] Lindholm LH, Ibsen H, Borch-Johnsen K, Olsen MH, Wachtell K, Dahlöf B, et al. Risk of new-onset diabetes in the losartan intervention for endpoint reduction in hypertension study. J Hypertens 2002;20:1879–86.
[11] Pfeffer MA, Swedberg K, Granger CB, Held P, McMurray JJ, Michelson EL, et al. Effects of candesartan on mortality and morbidity in patients with chronic heart failure: the CHARM-Overall programme. Lancet 2003;362:759–66.
[12] Julius S, Kjeldsen SE, Weber M, Brunner HR, Ekman S, Hansson L, et al. Outcomes in hypertensive patients at high cardiovascular risk treated with regimens based on valsartan or amlodipine: the VALUE randomised trial. Lancet 2004;363:2022–31.
[13] Tikellis C, Wookey PJ, Candido R, Andrikopoulos S, Thomas MC, Cooper ME. Improved islet morphology after blockade of the renin-angiotensin system in the ZDF rat. Diabetes 2004;53:989–97.
[14] Dhaunsi GS, Yousif MH, Akhtar S, Chappell MC, Diz DI, Benter IF. Angiotensin-(1-7) prevents diabetes-induced attenuation in PPAR-gamma and catalase activities. Eur J Pharmacol 2010;638:108–14.
[15] Benter IF, Yousif MH, Dhaunsi GS, Kaur J, Chappell MC, Diz DI. Angiotensin-(1-7) prevents activation of NADPH oxidase and renal vascular dysfunction in diabetic hypertensive rats. Am J Nephrol 2008;28:25–33.
[16] Benter IF, Yousif MH, Cojocel C, Al-Maghrebi M, Diz DI. Angiotensin-(1-7) prevents diabetes-induced cardiovascular dysfunction. Am J Physiol Heart Circ Physiol 2007;292:H666–72.
[17] Dharmani M, Mustafa MR, Achike FI, Sim MK. Effect of des-aspartate-angiotensin I on the actions of angiotensin II in the isolated renal and mesenteric vasculature of hypertensive and STZ-induced diabetic rats. Regul Pept 2005;129:213–9.
[18] Min L, Sim MK, Xu XG. Effects of des-aspartate-angiotensin I on angiotensin II-induced incorporation of phenylalanine and thymidine in cultured rat cardiomyocytes and aortic smooth muscle cells. Regul Pept 2000;95:93–7.
[19] Sim MK, Yuan HT. Effects of des-Asp-angiotensin I on the contractile action of angiotensin II and angiotensin III. Eur J Pharmacol 1995;278:175–8.
[20] Sim MK, Radhakrishnan R. Novel central action of des-Asp-angiotensin I. Eur J Pharmacol 1994;257:R1–3.
[21] Sim MK, Xu XG, Wong YC, Sim SZ, Lee KO. Des-aspartate-angiotensin I exerts hypoglycemic action via glucose transporter-4 translocation in type 2 diabetic KKAy mice and GK rats. Endocrinology 2007;148:5925–32.
[22] Keller S. Role of the insulin-regulated aminopeptidase IRAP in insulin action and diabetes. Biol Pharm Bull 2004;27:761–4.
[23] Keller S. The insulin-regulated aminopeptidase: a companion and regulator of GLUT4. Front Biosci 2003;8:s410–20.
[24] Yeh T, Sbodio J, Tsun Z, Luo B, Chi N. Insulin-stimulated exocytosis of GLUT4 is enhanced by IRAP and its partner tankyrase. Biochem J 2007;402:279–90.
[25] Martin S, Rice J, Gould G, Keller S, Slot J, James D. The glucose transporter GLUT4 and the aminopeptidase vp165 colocalise in tubulo-vesicular elements in adipocytes and cardiomyocytes. J Cell Sci 1997;110(Pt 18):2281–91.
[26] Ross S, Scott H, Morris N, Leung W, Mao F, Lienhard G, et al. Characterization of the insulin-regulated membrane aminopeptidase in 3T3-L1 adipocytes. J Biol Chem 1996;271:3328–32.
[27] Sumitani S, Ramlal T, Somwar R, Keller S, Klip A. Insulin regulation and selective segregation with glucose transporter-4 of the membrane aminopeptidase vp165 in rat skeletal muscle cells. Endocrinology 1997;138:1029–34.
[28] Farese R, Sajan M, Yang H, Li P, Mastorides S, Gower WJ, et al. Muscle-specific knockout of PKC-lambda impairs glucose transport and induces metabolic and diabetic syndromes. J Clin Invest 2007;117:2289–301.
[29] Ye L, Lee K, Su L, Toh W, Haider H, Law P, et al. Skeletal myoblast transplantation for attenuation of hyperglycaemia, hyperinsulinaemia and glucose intolerance in a mouse model of type 2 diabetes mellitus. Diabetologia 2009;52:1925–34.
[30] Zisman A, Peroni O, Abel E, Michael M, Mauvais-Jarvis F, Lowell B, et al. Targeted disruption of the glucose transporter 4 selectively in muscle causes insulin resistance and glucose intolerance. Nat Med 2000;6:924–8.
[31] Koh H, Arnolds D, Fujii N, Tran T, Rogers M, Jessen N, et al. Skeletal muscle-selective knockout of LKB1 increases insulin sensitivity, improves glucose homeostasis, and decreases TRB3. Mol Cell Biol 2006;26:8217–27.
[32] Matsuda M, DeFronzo R. Insulin sensitivity indices obtained from oral glucose tolerance testing: comparison with the euglycemic insulin clamp. Diabetes Care 1999;22:1462–70.
[33] Weigert C, Kron M, Kalbacher H, Pohl AK, Runge H, Häring HU, et al. Interplay and effects of temporal changes in the phosphorylation state of serine-302, -307, and -318 of insulin receptor substrate-1 on insulin action in skeletal muscle cells. Mol Endocrinol 2008;22:2729–40.
[34] Hansen PA, Han DH, Marshall BA, Nolte LA, Chen MM, Mueckler M, et al. A high fat diet impairs stimulation of glucose transport in muscle. Functional evaluation of potential mechanisms. J Biol Chem 1998;273:26157–63.
[35] Parekh P, Petro A, Tiller J, Feinglos M, Surwit R. Reversal of diet-induced obesity and diabetes in C57BL/6J mice. Metabolism 1998;47:1089–96.
[36] Opara E, Petro A, Tevrizian A, Feinglos M, Surwit R. L-glutamine supplementation of a high fat diet reduces body weight and attenuates hyperglycemia and hyperinsulinemia in C57BL/6J mice. J Nutr 1996;126:273–9.
[37] Collins S, Martin T, Surwit R, Robidoux J. Genetic vulnerability to diet-induced obesity in the C57BL/6J mouse: physiological and molecular characteristics. Physiol Behav 2004;81:243–8.
[38] Surwit R, Kuhn C, Cochrane C, McCubbin J, Feinglos M. Diet-induced type II diabetes in C57BL/6J mice. Diabetes 1988;37:1163–7.

[39] Surwit R, Feinglos M, Rodin J, Sutherland A, Petro A, Opara E, et al. Differential effects of fat and sucrose on the development of obesity and diabetes in C57BL/6J and A/J mice. Metabolism 1995;44:645–51.
[40] Wen Q, Sim MK, Tang FR. Reduction of infarct size by orally administered des-aspartate-angiotensin I in the ischemic reperfused rat heart. Regul Pept 2004;120:149–53.
[41] Sim MK, Min L. Effects of des-Asp-angiotensin I on experimentally-induced cardiac hypertrophy in rats. Int J Cardiol 1998;63:223–7.
[42] Kwoon SM, Ru TF, Guang XX. Effects of des-aspartate-angiotensin I on neointima growth and cardiovascular hypertrophy. Regul Pept 2004;117:213–7.
[43] Ng ET, Sim MK, Loke WK. Protective actions of des-aspartate-angiotensin I in mice model of CEES-induced lung intoxication. J Appl Toxicol 2010.
[44] Prada P, Zecchin H, Gasparetti A, Torsoni M, Ueno M, Hirata A, et al. Western diet modulates insulin signaling, c-Jun N-terminal kinase activity, and insulin receptor substrate-1ser307 phosphorylation in a tissue-specific fashion. Endocrinology 2005;146:1576–87.
[45] Hirosumi J, Tuncman G, Chang L, Gorgun CZ, Uysal KT, Maeda K, et al. A central role for JNK in obesity and insulin resistance. Nature 2002;420:333–6.
[46] Paolisso G, Tataranni PA, Foley JE, Bogardus C, Howard BV, Ravussin E. A high concentration of fasting plasma non-esterified fatty acids is a risk factor for the development of NIDDM. Diabetologia 1995;38:1213–7.
[47] Hotamisligil GS, Shargill NS, Spiegelman BM. Adipose expression of tumor necrosis factor-alpha: direct role in obesity-linked insulin resistance. Science 1993;259:87–91.
[48] Sim MK, Min L. Des-aspartate-angiotensin I and angiotensin AT1 receptors in rat cardiac ventricles. Regul Pept 2005;129:133–7.
[49] Chen WS, Sim MK. Effects of des-aspartate-angiotensin I on the expression of angiotensin AT1 and AT2 receptors in ventricles of hypertrophic rat hearts. Regul Pept 2004;117:207–12.
[50] de Carvalho-Filho MA, Carvalheira JB, Velloso LA, Saad MJ. Insulin and angiotensin II signaling pathways cross-talk: implications with the association between diabetes mellitus, arterial hypertension and cardiovascular disease. Arq Bras Endocrinol Metabol 2007;51:195–203.
[51] Diamond-Stanic M, Henriksen E. Direct inhibition by angiotensin II of insulin-dependent glucose transport activity in mammalian skeletal muscle involves a ROS-dependent mechanism. Arch Physiol Biochem 2010;116:88–95.
[52] Velloso L, Folli F, Sun X, White M, Saad M, Kahn C. Cross-talk between the insulin and angiotensin signaling systems. Proc Natl Acad Sci USA 1996;93:12490–5.
[53] Lee S, Harris N. Losartan and ozagrel reverse retinal arteriolar constriction in non-obese diabetic mice. Microcirculation 2008;15:379–87.
[54] Perico N, Ruggenenti P, Remuzzi G. Losartan in diabetic nephropathy. Expert Rev Cardiovasc Ther 2004;2:473–83.
[55] Paolisso G, Di Maro G, D'Amore A, Passariello N, Gambardella A, Varricchio M, et al. Low-dose iloprost infusion improves insulin action in aged healthy subjects and NIDDM patients. Diabetes Care 1995;18:200–5.
[56] Leighton B, Challiss RA, Newsholme EA. The role of prostaglandins as modulators of insulin-stimulated glucose metabolism in skeletal muscle. Horm Metab Res Suppl 1990;22:89–95.
[57] Bishop-Bailey D. Peroxisome proliferator-activated receptors in the cardiovascular system. Br J Pharmacol 2000;129:823–34.
[58] Wasner H, Weber S, Partke H, Amini-Hadi-Kiashar H. Indomethacin treatment causes loss of insulin action in rats: involvement of prostaglandins in the mechanism of insulin action. Acta Diabetol 1994;31:175–82.
[59] Krebs LT, Kramár EA, Hanesworth JM, Sardinia MF, Ball AE, Wright JW, et al. Characterization of the binding properties and physiological action of divalinal-angiotensin IV, a putative AT4 receptor antagonist. Regul Pept 1996;67:123–30.
[60] Albiston A, McDowall S, Matsacos D, Sim P, Clune E, Mustafa T, et al. Evidence that the angiotensin IV (AT(4)) receptor is the enzyme insulin-regulated aminopeptidase. J Biol Chem 2001;276:48623–6.
[61] Handa R. Biphasic actions of angiotensin IV on renal blood flow in the rat. Regul Pept 2006;136:23–9.
[62] Li X, Campbell D, Ohishi M, Yuan S, Zhuo J. AT1 receptor-activated signaling mediates angiotensin IV-induced renal cortical vasoconstriction in rats. Am J Physiol Renal Physiol 2006;290:F1024–33.
[63] Coleman J, Lee J, Miller J, Nuttall A. Changes in cochlear blood flow due to intra-arterial infusions of angiotensin II (3-8) (angiotensin IV) in guinea pigs. Hear Res 1998;119:61–8.
[64] Hamilton T, Handa R, Harding J, Wright J. A role for the angiotensin IV/AT4 system in mediating natriuresis in the rat. Peptides 2001;22:935–44.
[65] Shibata K, Kajiyama H, Ino K, Nawa A, Nomura S, Mizutani S, et al. P-LAP/IRAP-induced cell proliferation and glucose uptake in endometrial carcinoma cells via insulin receptor signaling. BMC Cancer 2007;7:15.
[66] Li Y, Block E, Patel J. Activation of multiple signaling modules is critical in angiotensin IV-induced lung endothelial cell proliferation. Am J Physiol Lung Cell Mol Physiol 2002;283:L707–16.
[67] Zhang J, Stobb J, Hanesworth J, Sardinia M, Harding J. Characterization and purification of the bovine adrenal angiotensin IV receptor (AT4) using [125I]benzoylphenylalanine-angiotensin IV as a specific photolabel. J Pharmacol Exp Ther 1998;287:416–24.
[68] Zhang J, Hanesworth J, Sardinia M, Alt J, Wright J, Harding J. Structural analysis of angiotensin IV receptor (AT4) from selected bovine tissues. J Pharmacol Exp Ther 1999;289:1075–83.
[69] Chi N, Lodish H. Tankyrase is a golgi-associated mitogen-activated protein kinase substrate that interacts with IRAP in GLUT4 vesicles. J Biol Chem 2000;275:38437–44.